Disulfide Bond Isomerization in BPTI and BPTI(G36S): An NMR Study of Correlated Mobility in Proteins†

Gottfried Otting, Edvards Liepinsh, and Kurt Wüthrich*

Institut für Molekularbiologie und Biophysik, Eidgenössische Technische Hochschule-Hönggerberg, CH-8093 Zürich, Switzerland

Received November 19, 1992; Revised Manuscript Received January 22, 1993

ABSTRACT: Two conformational isomers were observed in the ^{1}H nuclear magnetic resonance (NMR) spectra of the basic pancreatic trypsin inhibitor (BPTI) and of a mutant protein with Gly 36 replaced by Ser, BPTI(G36S). The less abundant isomer differs from the major conformation by different chirality of the Cys 14–Cys 38 disulfide bond. In BPTI, the population of the minor conformer increases from about 1.5% at 4 °C to 8% at 68 °C. In BPTI(G36S), the population of the minor conformation is about 15% of the total protein, so that a detailed structural study was technically feasible; a trend toward increasing population of the minor conformer at higher temperatures was observed also for this mutant protein. The activation parameters for the exchange between the two conformations were measured in the temperature range 4–68 °C, using uniformly ^{15}N-enriched protein samples. Below room temperature the exchange rate of the disulfide flip follows an Arrhenius-type temperature dependence, with negative activation entropy in both proteins. At higher temperatures the exchange rates are governed by a different set of activation parameters, which are similar to those for the ring flips of Tyr 35 about the C^β–C^γ bond. Although the equilibrium enthalpy and entropy were found to be largely temperature independent, the activation entropy changes sign and is positive at higher temperatures. These results suggest that, above room temperature, the disulfide flips are coupled to the same protein structure fluctuations as the ring flips of Tyr 35.

BPTI[1] is among the best characterized and most thoroughly investigated of all proteins. Three high-resolution crystal structures are available (Deisenhofer et al., 1975; Wlodawer et al., 1984, 1987), and a high-quality structure has been determined by NMR in aqueous solution (Berndt et al., 1992). Furthermore, the dynamic properties of BPTI in solution were extensively investigated by NMR (Wagner, 1980; Richarz et al., 1980; Wagner et al., 1984; Wagner & Nirmala, 1989), and there is a large body of data on structural effects of chemical modifications and site-directed mutagenesis (e.g., Kress et al., 1968; Wagner et al., 1984; Chazin et al., 1985; Vanmierlo et al., 1991). On the basis of this wealth of data, observations on subtle localized variations of structure and dynamics can now be made with BPTI, although similar effects might escape detection in other proteins. In the present study, investigations of the mutant BPTI(G36S) lead to the discovery of a slow dynamic equilibrium between two conformers with different chirality of the disulfide bridge formed by Cys 14 and Cys 38. The same two-state equilibrium was then also found in wild-type BPTI.

In BPTI(G36S), the hydroxyl-bearing side chain of Ser 36 replaces the internal water molecule that is present in a cavity formed between the peptide segments of residues 11–14 and 35–38 of the wild-type BPTI structure (Berndt et al., 1993). Amide proton exchange experiments and NOESY spectra recorded at 4 °C with BPTI(G36S) and BPTI indicated that the backbone conformation and the hydrogen-bonding network are virtually unaltered by the mutation, but more significant differences were observed at 36 °C. It had been noted earlier in wild-type BPTI that some proton resonances in the polypeptide segment 14–18 are broadened at 36 °C, and in the past only few NOEs with these resonances could be identified (Wagner & Wüthrich, 1982; Wagner et al., 1987; Berndt et al., 1992). Furthermore, increased transverse ^{13}C relaxation rates were observed for the α-carbon resonances of Cys 14 and Cys 38 (Wagner & Nirmala, 1989). These data, together with the observation of pronounced intensity changes of the COSY cross-peaks with temperature, have previously led to the conclusion that increased internal mobility prevailed in this part of the molecule (Wagner et al., 1987; Wagner & Nirmala, 1989). In BPTI(G36S), these dynamic effects could now be studied in more detail and characterized by an equilibrium between distinct, different molecular conformations.

In earlier work, slow local conformational equilibria in peptides and proteins were shown to involve cis–trans isomerization of Xxx–Pro peptide bonds (Grathwohl & Wüthrich, 1981) and 180° flips of aromatic rings about the C^β–C^γ bond (Wüthrich 1976, 1986). In the strongly constrained *cyclo*-L-cystine, slow chemical exchange has also been observed between two conformations that differ by the chirality of the disulfide bond (Donzel et al., 1972; Jung & Ottnad, 1974), and a similar exchange process was detected for the sterically constrained disulfide bridge in a cyclic octapeptide (Kopple et al., 1988). X-ray analyses of different crystal forms of proteins and peptides occasionally showed the occurrence of isoforms with different disulfide bond chiralities (Richardson, 1981). In addition to the experimental evidence for the presence of two BPTI conformations with different disulfide bond chirality, the present article presents a detailed investigation of the temperature dependence of the equilibrium constants and the interconversion rates between the two conformations in BPTI and BPTI(G36S). The kinetic analysis

† This work was supported by the Schweizerischer Nationalfonds (Project Nr. 31.32033.91).

[1] Abbreviations: BPTI, bovine pancreatic trypsin inhibitor; BPTI(G36S), BPTI with glycine in position 36 replaced by serine; NMR, nuclear magnetic resonance; COSY, two-dimensional correlated spectroscopy; 2QF, two-quantum filtered; TOCSY, two-dimensional total correlation spectroscopy; NOE, nuclear Overhauser enhancement; NOESY, two-dimensional NOE spectroscopy in the laboratory frame; ROESY, two-dimensional NOE spectroscopy in the rotating frame; TPPI, time-proportional phase incrementation.

0006-2960/93/0432-3571$04.00/0

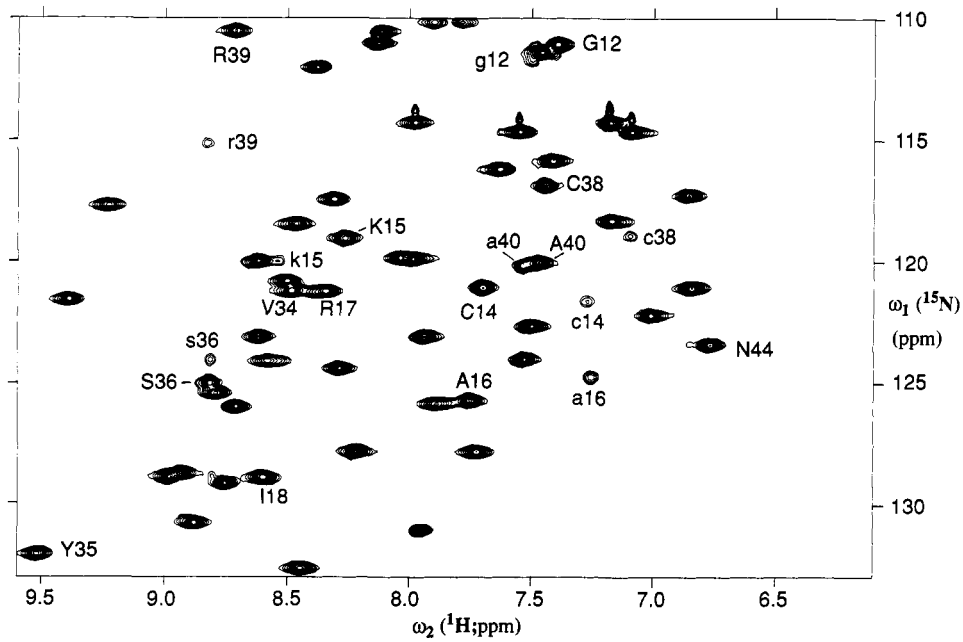

FIGURE 1: Region [ω_1(^{15}N) = 110–133 ppm, ω_2(^{1}H) = 6.2–9.6 ppm] of a [^{15}N,^{1}H]-COSY spectrum recorded with a 20 mM solution of uniformly ^{15}N-labeled BPTI(G36S) in 90% H_2O/10% ^2H_2O, pH 4.6, T = 10 °C. Spectral parameters used: t_{1max} = 72 ms, t_{2max} = 144 ms, recorded data size 800 × 2048 points, ^{1}H frequency = 600 MHz, and total recording time about 9 h. The cross-peaks of the amide groups with different chemical shifts in the major and minor conformations (see text) are identified with the one-letter amino acid symbol and the sequence number, where the cross-peaks of the minor conformation are labeled with lowercase letters. The minor peaks of Arg 17, Ile 18, Val 34, and Tyr 35 are clearly visible in the experiment of Figure 2.

of the disulfide bond isomerization gives new insights into mutual coupling of different modes of internal structure fluctuations in BPTI.

MATERIALS AND METHODS

Uniformly ^{15}N-enriched BPTI and BPTI(G36S) were obtained as a gift from Bayer A.G., Leverkusen, Germany. The preparation of these recombinant proteins was recently described elsewhere (Berndt et al., 1993). Due to the overexpression system used, both proteins contain an extra methionyl residue in position 0, i.e., amino-terminal of the regular amino acid sequence. Since in both the primary structure and the three-dimensional structure the amino terminus is well separated from the mutation site at residue 36, we refer to the otherwise unmutated BPTI sample from the overexpression system as "wild-type BPTI".

NMR spectra were recorded with 20 mM protein solutions at pH 4.6 either in 90% H_2O/10% ^2H_2O or in 100% ^2H_2O on Bruker AMX 500 and AMX 600 NMR spectrometers. [^{15}N,^{1}H]-COSY experiments were performed with the pulse scheme of Bodenhausen and Ruben (1980) using a spin-lock purge pulse for water suppression (Otting & Wüthrich, 1988; Messerle et al., 1989). A 2QF-COSY spectrum (Rance et al., 1983) and clean-TOCSY (Griesinger et al., 1988) and ROESY spectra (Bothner-By et al., 1984) with short mixing times were recorded with BPTI(G36S) in D_2O solution at 4 °C for the purpose of obtaining spectral assignments. Furthermore, NOESY and ROESY spectra of native BPTI recorded previously at 4, 36, 50, and 68 °C using a mixing time of 112 ms (Otting & Wüthrich, 1989) were used to collect some of the information reported here.

Quantitative exchange rates between the two protein conformations present in equilibrium were obtained with the [^{15}N,^{1}H]-two-spin-order-exchange difference experiment (Wider et al., 1991). The two data files recorded with the mixing time, τ_{mix}, inserted before or after the t_1-evolution period, respectively, were obtained in an interleaved manner and stored separately. For BPTI(G36S), each recording of a difference spectrum took between 1.7 and 3 h. To enable observation of the minor conformation, which is present at very low concentrations, the exchange experiments with BPTI were recorded using about 44 h per difference spectrum.

RESULTS

Experimental Evidence for the Presence of Two Protein Conformations in Equilibrium. Figure 1 shows the spectral region of the [^{15}N,^{1}H]-COSY spectrum of BPTI(G36S) at 10 °C that contains the ^{15}N–^{1}H cross-peaks of the backbone amide groups. In addition to a complete fingerprint (Wüthrich, 1986) of strong peaks, several signals of a less abundant protein species are observed. The exchange cross-peaks observed in the difference spectrum of the [^{15}N,^{1}H]-two-spin-order exchange experiment (Figure 2) (Wider et al., 1991) show that this minor species undergoes exchange with the main component: a characteristic rectangular cross-peak pattern is observed for each pair of exchanging resonances; the exchange cross-peak pattern is observed for each pair of exchanging resonances; the exchange cross-peaks are of opposite sign than the direct [^{15}N,^{1}H]-COSY cross-peaks, which were identified by comparison with the spectrum of Figure 1. Since the direct cross-peaks are largely suppressed in the difference spectrum (Wider et al., 1991), the rectangular exchange pattern can also be observed for some amino acid residues where the chemical shift differences between the minor and major conformers are too small for the peaks to be resolved in the conventional [^{15}N,^{1}H]-COSY spectrum (Figure 1). Examples are the exchange patterns of Arg 17, Ile 18, Val 34, and Tyr 35 (Figure 2). With only few exceptions, Figure 2 contains exchange cross-peaks for all the residues 12–18 and 35–40. The exceptions are Pro 13, which has no amide proton, Ser 36, for which the exchange cross-peaks and the direct cross-peaks coincide due to degenerate amide proton chemical shifts in the two conformers (Figure 1), and Gly 37, for which the exchange pattern was observed outside the spectral region shown in Figures 1 and 2.

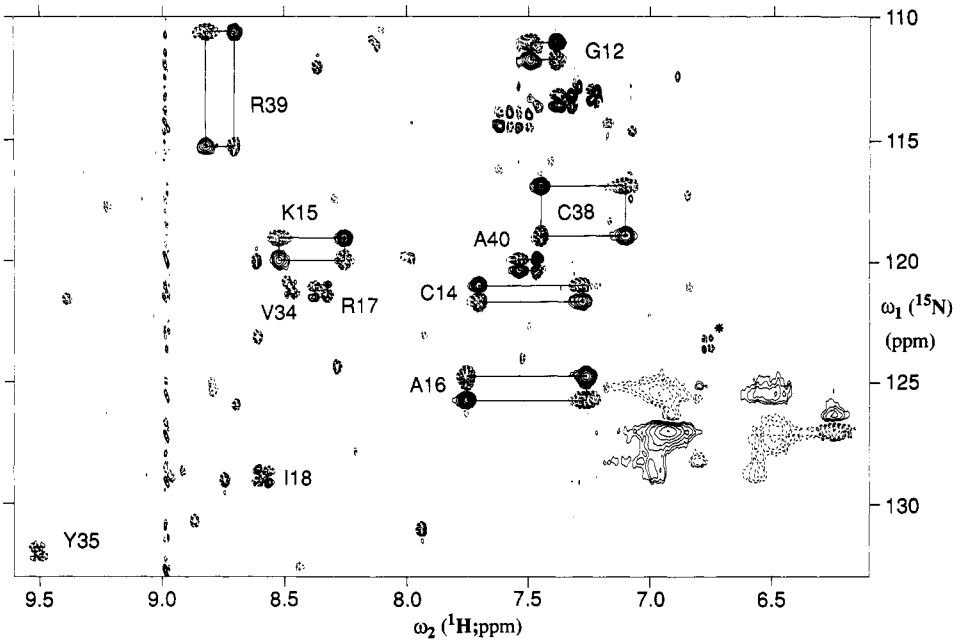

FIGURE 2: Same spectral region as in Figure 1 of the difference spectrum from a [^{15}N,^{1}H]-two-spin-exchange experiment (Wider et al., 1991) with BPTI(G36S). The same sample and same temperature are used as in Figure 1. Spectral parameters used: mixing time 25 ms, t_{1max} = 40 ms, t_{2max} = 144 ms, recorded data size 128 × 2048 points, ^{1}H frequency = 600 MHz, and total recording time about 4 h. States–TPPI quadrature detection with delayed acquisition was used in the ω_1 dimension (Marion et al., 1989; Bax et al., 1991), resulting in folding of the cross-peaks from the guanidium groups of the arginyl side chains into the spectral regions near ($\omega_1 \approx 127$ ppm, $\omega_2 \approx 6.7$ ppm) and near ($\omega_1 \approx 114$ ppm, $\omega_2 \approx 7.4$ ppm). Positive and negative levels were plotted with broken and solid lines, respectively, where the exchange cross-peaks connecting the direct ^{15}N–^{1}H cross-peaks of the major and minor conformers are positive. The rectangular patterns formed by two negative, direct COSY cross-peaks and by two positive exchange cross-peaks (Wider et al., 1991) are identified with solid lines, the amino acid one-letter symbol, and the sequence number of the exchanging residue. Additional positive signals that are not part of an exchange pattern arise from incomplete cancellation of [^{15}N,^{1}H]-COSY cross-peak intensity in the difference spectrum. The asterisk identifies an apparent exchange peak pattern at the position of Asn 44 (Figure 1).

Additional exchange cross-peaks for the NH_2 protons of the arginyl side chains arise from 180° flips about the N^{ϵ}–C^{ζ} bond of the guanidinium groups. These cross-peaks are in principle outside the spectral region shown in Figure 2 but appear at about (ω_1 = 127 ppm, ω_2 = 6.7 ppm) because the spectrum has been folded in the ω_1 dimension to reduce the recording time. Similarly, residual intensity due to incomplete cancellation of the intense direct cross-peaks of the ϵNH groups of the arginyl side chains is folded into positions near (ω_1 = 114 ppm, ω_2 = 7.4 ppm) (Figure 2).

At 13 °C the less abundant conformation of BPTI amounts to only about 2% of the total protein concentration. Therefore, the intensities of the signals from the minor conformation in a [^{15}N,^{1}H]-COSY spectrum (not shown) are of similar intensity as those of small amounts of protein impurities present in the sample preparation used. The signals from the minor conformation could thus be unambiguously identified only in the difference spectrum of the [^{15}N,^{1}H]-two-spin-order-exchange experiment (Figure 3). Figure 3 shows that in BPTI the same amino acid residues give rise to discernible exchange cross-peaks as in BPTI(G36S). The only differences are observed for Val 34 and Tyr 35, which have only weak exchange patterns in BPTI(G36S) (Figure 2) and give no exchange peaks in BPTI, and for position 36. Gly 36 in BPTI gives rise to exchange cross-peaks (Figure 3), whereas no exchange peaks are observed for Ser 36 in BPTI(G36S) (Figure 2) because of the degeneracy of the amide proton chemical shifts in the two conformations (Figure 1).

Conformational Studies of the Less Abundant Form of the Proteins. Two factors interfered with an extensive collection of NOE distance constraints for a structure determination of the minor conformation. First, for both BPTI and BPTI-(G36S) the exchange with the more abundant conformation caused much stronger cross-peaks than those originating from NOEs between different protons of the minor conformation. For example, TOCSY and NOESY spectra recorded at 4 °C with mixing times of 60 ms showed strong exchange cross-peaks between corresponding diagonal peaks of the two conformers but only very weak intramolecular NOE cross-peaks of the minor conformation, because the magnetization of the latter relaxed rapidly into magnetization of the major conformation during the time period between evolution and detection. Effects of this relaxation pathway could only be suppressed by the use of very short mixing times. Second, for BPTI there was the additional difficulty that the abundance of the minor conformation is only of the order of 2% of the total protein concentration. As a consequence, we first concentrated on studies of BPTI(G36S) with experiments using very short mixing times and then transferred some of the results obtained with BPTI(G36S) to BPTI by systematic comparison of corresponding ^{15}N and ^{1}H chemical shifts, which are well known to respond sensitively to conformational differences (Wüthrich, 1976, 1986).

As a basis for collecting the desired local structural information, it was crucial to obtain stereospecific assignments for βCH_2 of Cys 14 and Cys 38. Figure 4 shows the region of a ROESY spectrum recorded in D_2O solution with a mixing time of 8 ms, which contains the β_2H–β_3H cross-peaks of Cys 14 and Cys 38 for both conformations. Even with this short mixing time, exchange cross-peaks are observed between the corresponding β_2H–β_3H cross-peaks of the major and minor conformations, where the exchange cross-peaks of Cys 14 have the same sign as the negative direct ROE cross-peaks, whereas positive exchange cross-peaks are observed for Cys 38 (see below). These exchange cross-peaks enabled the transfer of stereospecific resonance assignments between corresponding βCH_2 groups in the major and minor conformations.

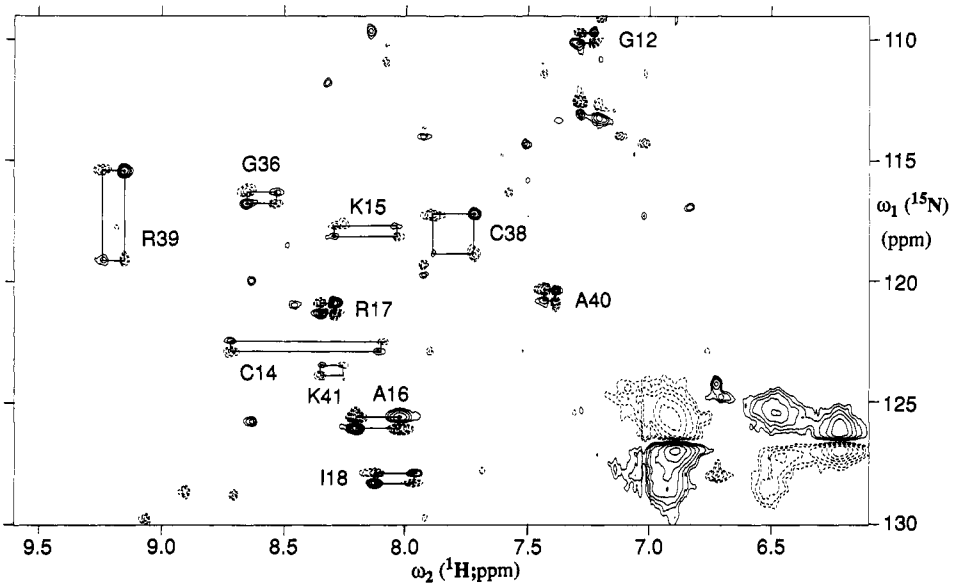

FIGURE 3: Spectral region [ω_1(^{15}N) = 109–130 ppm, ω_2(^{1}H) = 6.1–9.6 ppm] from the difference spectrum of a [^{15}N,^{1}H]-two-spin-exchange experiment with a 20 mM solution of uniformly ^{15}N-labeled BPTI in 90% H_2O/10% ^2H_2O at pH 4.6, T = 13 °C. Spectral parameters used: mixing time = 10 ms, t_{1max} = 40 ms, t_{2max} = 144 ms, recorded data size 256 × 2048 points, ^{1}H frequency = 600 MHz, and total recording time 44 h. The presentation is the same as in Figure 2. The spectrum also contains folded peaks of the Arg side chains in similar positions as in Figure 2.

At first, stereospecific resonance assignments were established in the major conformation, using the assumption that the major solution conformation around the Cys 14–Cys 38 disulfide bridge in BPTI(G36S) is identical to the crystal structures of native BPTI (Deisenhofer & Steigemann, 1975; Wlodawer et al., 1984, 1987). This assumption was based on the near identity of the structures of BPTI in solution and in crystals (Berndt et al., 1992) and on the close similarity of corresponding chemical shifts, NOE intensities, and spin–spin coupling constants in BPTI(G36S) and BPTI. Furthermore, the NOEs and spin–spin coupling constants involving hydrogen atoms of the residues near the Cys 14–Cys 38 disulfide bond in BPTI(G36S) are in full agreement with predictions based on the BPTI crystal structures: (i) In the crystal structure of BPTI, the β_2- and β_3-protons of Cys 14 are, respectively, trans and gauche with respect to the α-proton, with the amide proton of Lys 15 closer to the β_3-proton. Correspondingly, the β-proton resonances at high field and low field have αH–βH COSY cross-peak patterns indicative of a big and a small scalar coupling constant $^3J_{\alpha\beta}$, respectively. The low-field resonance shows a much stronger NOE with the α-proton of Cys 14 and with the amide proton signal of Lys 15 (not shown). The ensuing assignment of the high-field resonance to β_2 coincides with the stereospecific resonance assignments in wild-type BPTI (Berndt et al., 1992). (ii) For Cys 38, both β-protons are gauche with respect to the α-proton, with the amide proton of Arg 39 closer to the β_2-proton. As predicted from this local feature of the crystal structure, the αH–βH COSY cross-peak multiplets of the major conformation in BPTI(G36S) manifest small scalar coupling constants $^3J_{\alpha\beta}$ for both β-protons. The β-proton resonance at lower field shows a much stronger NOE with the amide proton of Arg 39 and was therefore assigned to the β_2-proton. The same result was obtained with wild-type BPTI, except that the sequential NOE between the lower field β-proton of Cys 38 and the amide proton of Arg 39 could be resolved only at temperatures above 50 °C. Therefore, no stereospecific resonance assignment of the β-protons of Cys 38 was used in the recent refinement of the NMR structure of BPTI, which was carried out at 36 °C (Berndt et al., 1992).

From the stereospecific assignments of the βCH_2 resonances of Cys 14 and Cys 38 in the major conformer the corresponding assignments for the minor conformer were obtained from the sign of the exchange cross-peaks in Figure 4. Figure 5 outlines schematically the cross-peak patterns observed for Cys 14 and Cys 38. There are three classes of cross-peaks present:

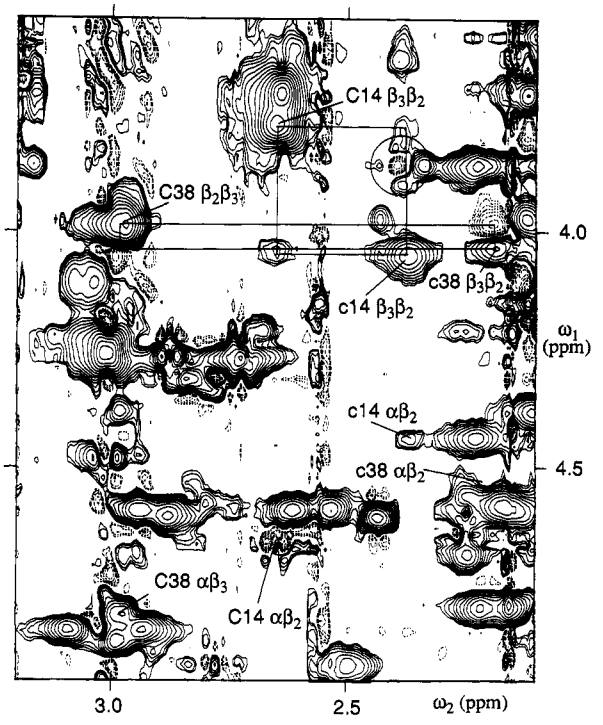

FIGURE 4: Region (ω_1 = 3.6–4.9 ppm, ω_2 = 2.1–3.2 ppm) of a [^{1}H,^{1}H]-ROESY spectrum recorded with a 20 mM solution of BPTI(G36S) in ^2H_2O, p^{2}H 4.6, T = 4 °C. Spectral parameters used: mixing time τ_m = 8 ms, t_{1max} = 50 ms, t_{2max} = 144 ms, recorded data size 700 × 2048 points, ^{1}H frequency = 600 MHz, and total recording time 52 h. Positive and negative levels were plotted with broken and solid lines, respectively. The positions of the intraresidual ROE cross-peaks of Cys 14 and Cys 38 are labeled with the same symbols as in Figure 1, where in addition the protons observed in the ω_1 and ω_2 dimensions are identified by the first and second Greek letter, respectively. Two rectangles connect ROE cross-peaks of the major and minor conformers of Cys 38 and Cys 14 with the respective exchange cross-peaks (see the text and Figure 5). A circle is drawn around a J cross-peak (Macura et al., 1982) that overlaps with an exchange cross-peak of Cys 14.

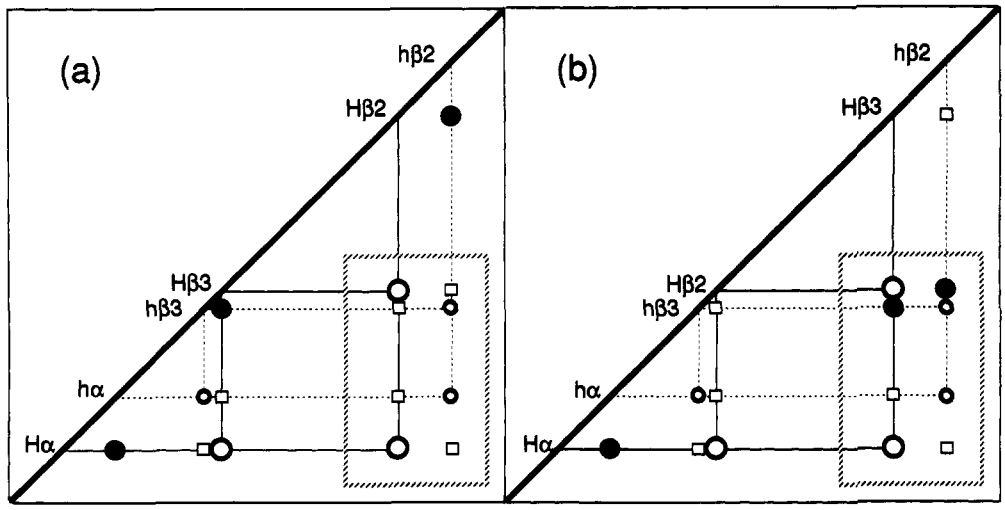

FIGURE 5: Schematic representation of the [^{1}H,^{1}H]-ROESY cross-peak patterns observed for (a) Cys 14 and (b) Cys 38. Upper- and lowercase characters along the diagonal identify the chemical shifts of the hydrogen atoms indicated with greek letters and numbers for the major and minor conformations, respectively. Open circles represent negative direct ROE cross-peaks, filled circles positive chemical exchange cross-peaks, and squares negative exchange-relayed ROE cross-peaks. Solid lines connect the diagonal peaks and cross-peaks observed for the major conformation, broken lines those of the minor conformation. The dashed rectangles correspond to the spectral region shown in Figure 4.

(i) Negative peaks representing direct ROEs (Bothner-By et al., 1984) (open circles); (ii) positive peaks representing chemical exchange (filled circles); (iii) negative peaks representing exchange-relayed ROE cross-peaks (open squares), which arise from magnetization transfer via a single ROE step followed by chemical exchange, or via chemical exchange followed by a single ROE step. For Cys 14 (Figure 5a), the chemical shift differences between corresponding resonances of the major and minor conformers are small, and therefore all positive chemical-exchange cross-peaks are close to the diagonal. The spectral region shown in Figure 4 contains exclusively negative ROE cross-peaks and exchange-relayed ROE cross-peaks of Cys 14. For Cys 38 (Figure 5b), the chemical shifts of the β_2H and β_3H resonances of the major and minor conformations are largely different. As a result, the positive chemical-exchange cross-peaks between corresponding β-protons are well separated from the diagonal. They are identified in Figure 4 by lines connecting them with the β_2H–β_3H cross-peak of Cys 38 in the major conformation and the corresponding β_3H–β_2H cross-peak in the minor conformation. The exchange-relayed ROE cross-peaks between αH and βCH$_2$ (Figure 5b) are not observed in Figure 4 because the αH–βH ROEs are much weaker than the ROEs between the geminal β-protons. The large differences between chemical shifts of corresponding hydrogen atoms in the two conformations point to direct involvement of the side chain of Cys 38 in the observed conformational rearrangement.

The aforementioned implications that the side chain orientations in the two conformations are similar for Cys 14 and different for Cys 38 are confirmed by a 2QF-COSY spectrum of BPTI(G36S) at 4 °C (Figure 6). The multiplet fine structure of the αH–β_2H cross-peaks of Cys 14 shows a large active coupling constant $^3J_{\alpha\beta_2}$ in both the minor and major conformations, which indicates that in both conformations the β_2-proton is in the trans orientation relative to the α-proton. The presence of a large and a small $^3J_{\alpha\beta}$ coupling constant for Cys 14 in both conformations is further inferred by the observation of strong and weak cross-peaks for, respectively, the αH–β_2H and αH–β_3H connectivities in a TOCSY spectrum recorded with a mixing time of 10 ms (not shown). A large $^3J_{\alpha\beta}$ coupling was then also indicated by the appearance at (ω_1 = 4.5 ppm, ω_2 = 2.2 ppm) in Figure 6 of the αH–β_2H COSY cross-peak of Cys 38 in the minor conformation. This cross-peak is of similar intensity as the

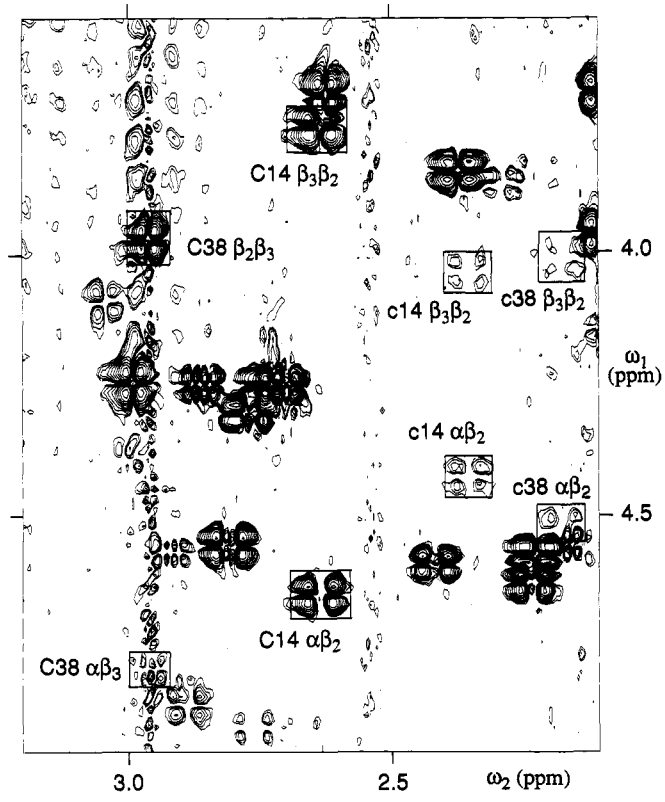

FIGURE 6: Homonuclear ^{1}H 2QF-COSY spectrum of a 10 mM solution of BPTI(G36S) in ^2H_2O, p^{2}H 4.6, T = 4 °C. Spectral parameters used: t_{1max} = 72 ms, t_{2max} = 144 ms, recorded data size 1024 × 2048 points, ^{1}H frequency = 6000 MHz, and total recording time 26 h. Positive and negative levels were plotted without distinction. The spectral region and symbols for cross-peak identification are the same as in Figure 4.

αH–β_3H cross-peak of Cys 38 in the major conformation, which is relatively weak due to the small value of $^3J_{\alpha\beta_3}$. These observations are again in line with the relative cross-peak intensities observed in the aforementioned TOCSY spectrum (not shown). The combined evidence from the chemical shift changes and the $^3J_{\alpha\beta}$ coupling constants shows that the local conformation of Cys 14 does not change significantly between the major and minor conformations, whereas a change of the χ^1 angle by about −120° is indicated for Cys 38, corresponding to a change from a gauche–gauche conformation in the major

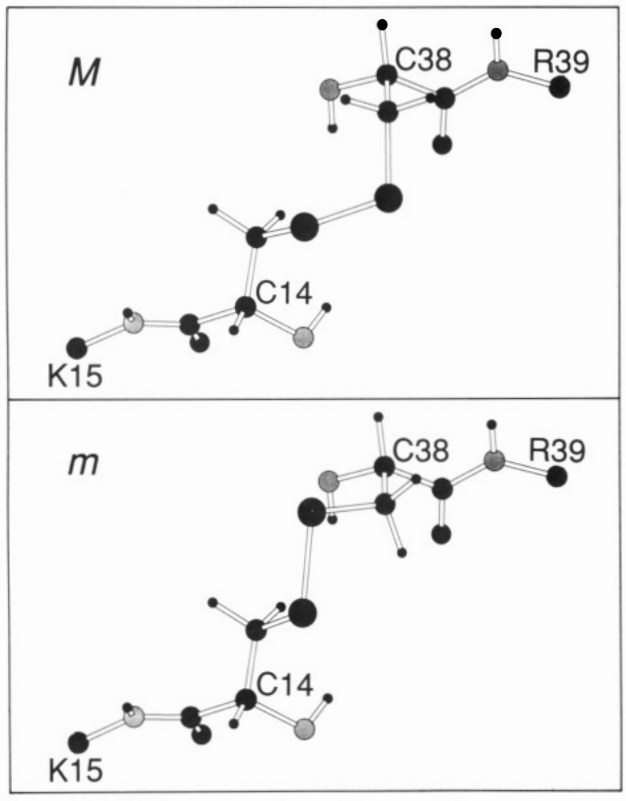

FIGURE 7: Model representations of the two different Cys 14–Cys 38 disulfide bond arrangements in the major and minor conformations of BPTI and BPTI(G36S). (M) More abundant species with right-handed chirality of the disulfide bridge. The atom coordinates were taken from the crystal structure of BPTI form II (Wlodawer et al., 1984). (m) Minor species with left-handed chirality of the disulfide bridge. The atom coordinates are the same as in M, except that relative to M the coordinates of the β-protons and the sulfur atom of Cys 38 were changed by a rotation of about –120° about the C^{α}–C^{β} bond. Atom code: carbon, black; oxygen, dark shaded; nitrogen, light-shaded; sulfur, big and dark-shaded; hydrogen, small and dark shaded. The α-carbons are labeled with the one-letter amino acid symbol and the sequence location.

conformer (Wagner et al., 1987) to a trans–gauche conformation in the less abundant conformer.

Figure 7 shows the two forms of the Cys14–Cys38 disulfide bridge which are implicated by the change of the χ^1 angle of Cys 38 from 60° in the major conformation to about –60° in the minor conformation. The disulfide bridge of the major conformation is the same as in the crystal structure and has a right-handed chirality (Figure 7a). In the minor conformation the disulfide bridge must assume a left-handed chirality, since the conformational change is restricted to the side chain of Cys 38 and the disulfide bond (Figure 7b). It is intriguing to note for Cys 38 that the chemical shift of the β_3-proton in the minor conformation is nearly the same as the chemical shift of the β_2-proton in the major conformation, since Figure 7 shows that these hydrogen atoms are in similar positions with respect to the framework provided by the parts of the protein that do not vary between the two conformations.

No evidence was obtained for further important conformational rearrangements. Table I lists the chemical shift differences between the major and minor conformations for all proton resonances in BPTI(G36S) for which resonance assignments are available in the minor conformation. It is seen that chemical shift changes larger than 0.2 ppm for carbon-bound protons occur exclusively in Cys 14 and Cys 38. The chemical shift change of the hydroxyl-proton of Ser 36 by 0.34 ppm could not be related to a significant conformational change of the side chain of Ser 36, since similar relative NOESY and TOCSY cross-peak intensities were

Table I: Chemical Shift Differences, $\Delta\delta = \delta_m - \delta_M$, between the ^1H Resonances of the Minor and Major Conformations of BPTI(G36S) at $T = 4$ °C and pH 4.6[a]

	$\Delta\delta$ (ppm)			
residue	NH	αH	βH	others
Gly 12	0.10	–0.02, 0.19		
Pro 13		–0.10		
Cys 14	–0.43	–0.22	–0.18, 0.28	
Lys 15	0.26	0.01		
Ala 16	–0.50	–0.09	–0.02	
Arg 17	0.05			
Ile 18	–0.01			
Val 34	0.01			
Tyr 35	–0.01			
Ser 36	0.00	0.08	0.03, –0.05	γOH 0.34
Gly 37	–0.03	0.05, –0.15		
Cys 38	–0.34	–0.26	1.06, –1.81	
Arg 39	0.12	0.03	–0.07	
Ala 40	0.07			

[a] Only those residues are listed for which resonance assignments could be obtained for the less abundant conformation.

observed with all side chain proton resonances of Ser 36 in both conformations, including the NOEs with the side chain hydroxyl proton (in these measurements special care was exercised to avoid any bias from spin diffusion by using short mixing times of 25 ms for NOESY and 10 ms for TOCSY). Amide proton chemical shifts are generally very sensitive to even minor changes in the chemical environment (Wüthrich, 1976). In the presently investigated system the amide proton chemical shift changes observed between major and minor conformation (Table I) are comparable to those between BPTI and BPTI(G36S) (Figures 2 and 3). We therefore conclude that there is no indication of major conformational changes in the amide proton chemical shift data.

The low abundance of the minor conformation in solutions of wild-type BPTI makes it difficult to observe any ^1H–^1H cross-peaks of this minor form in homonuclear COSY or ROESY spectra (Figures 4 and 6), so that only the ^{15}N–^1H cross-peaks could be assigned for the minor conformation. However, close similarity between the minor forms of BPTI and BPTI(G36S) is inferred from the following chemical shift analysis. The amide proton and amide ^{15}N chemical shifts of the major conformations of BPTI and BPTI(G36S) differ by up to 1.1 and 5.0 ppm, respectively (Figures 2 and 3). However, all large chemical shift differences between the major forms of the two proteins are with amide groups near the mutation site. Most important, the differences in chemical shifts between the major and minor conformations of the same protein are very similar for all ^1H and ^{15}N spins of the amide groups in BPTI and BPTI(G36S) (Figure 8). The only exceptions are some amide proton chemical shift differences observed for the residues 35–40, which may be explained by the fact that the interior water molecule present near Cys 38 in BPTI is likely to respond differently to the conformational change of the side chain of Cys 38 than the covalently bound $-CH_2-OH$ side chain of Ser 36 in BPTI(G36S) (Berndt et al., 1993).

Further evidence for close similarity of the conformations of BPTI and BPTI(G36S) was obtained from the β-proton chemical shifts of Cys 14 and Cys 38. The β_2H and β_3H resonances of Cys 38 in the minor conformation in BPTI-(G36S) are shifted, respectively, by –1.8, and +1.1 ppm relative to the corresponding chemical shifts in the major conformation, whereas the β-proton chemical shifts of Cys 14 differ by less than 0.3 ppm between the two forms (Figures 5 and 6). The presence of similar chemical shift differences of the corresponding protons in BPTI is implicated by the temperature

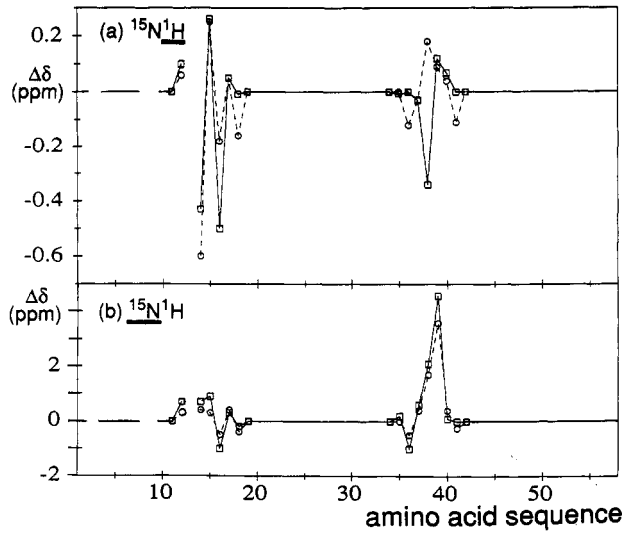

FIGURE 8: Plots of the chemical shift differences between the minor and major conformations of BPTI (squares connected by solid lines) and BPTI(G36S) (circles connected by dashed lines) at 10 °C, pH 4.6, versus the amino acid sequence. (a) Chemical shift differences of the amide protons. (b) Chemical shift differences of the amide ^{15}N spins.

dependence of the β-proton chemical shifts. Monitoring the β_2H–β_3H cross-peaks in NOESY spectra as a function of temperature, we found that the chemical shifts of the β_2H and β_3H resonances of Cys 38 changed by only about 0.01 ppm between 4 and 36 °C, whereas shifts of about −0.15 and +0.09 ppm, respectively, occurred between 36 and 68 °C. Furthermore, both β-proton resonances of Cys 38 are much broader between 50 and 68 °C than the β-proton signals of any of the other amino acid residues (see also the following section below). These observations can be explained by the facts that only the resonances of the major conformation of BPTI are seen between 4 and 36 °C and that there is coalescence with the signals of the minor form at higher temperatures. The chemical shifts of the coalesced lines correspond closely to those predicted from the chemical shifts of the major conformation of BPTI measured at 36 °C and those estimated for the minor conformation of BPTI with the assumption that they are similar to the corresponding shifts in BPTI(G36S). In contrast to the situation encountered with Cys 38, the line widths and chemical shifts of the β-proton resonances of Cys 14 in BPTI change only little with temperature. This again is what one would predict from the assumption that similar small chemical shift differences between the major and minor conformations prevail in BPTI and in BPTI(G36S).

Overall, the available data provide strong evidence that the minor conformation of BPTI comes about by a rearrangement of the disulfide bridge Cys14–Cys38, which would, in complete analogy with BPTI(G36S), include changes of the χ^1 angle of the Cys 38 and of the chirality of the disulfide bond. This conclusion is further corroborated by the fact that similar values were obtained for the activation enthalpies of the disulfide isomerization in the two proteins (see below).

Equilibrium Constants between the Major and Minor Conformations of BPTI and BPTI(G36S). All available data indicate that there is a two-state equilibrium between the major conformation, M, and the minor conformation, m (Figure 7):

$$\mathrm{M} \underset{k_m}{\overset{k_M}{\rightleftharpoons}} \mathrm{m} \qquad (1)$$

k_M and k_m are the rate constants of the conformational exchange. In the temperature range of slow exchange, the relative populations of the two conformations could be measured from the cross-peak intensities observed in the [^{15}N,^1H]-COSY spectra (Figure 1). At 4 °C, the minor conformations of BPTI(G36S) and BPTI were thus found to be populated in the extent of 14.4 ± 2.0% and 1.5 ± 0.3%, respectively, of the total protein.

At temperatures above the coalescence temperature of the signals of the two isomeric forms, the relative populations were determined by an analysis of chemical shifts and line widths. In BPTI(G36S), the β_2- and β_3-proton resonances of Cys 38 in the major conformation broaden at 50 °C and become narrower again at 68 °C, indicating that in this temperature range these resonances merge with those of the minor conformation. Since for Cys 14 the chemical shift differences of βCH_2 between the major and minor conformations are much smaller, the coalescence temperature is lower than for Cys 38 and the signals are narrow at both 50 and 68 °C. On the basis of comparison of the chemical shifts of the averaged signals at 68 °C with those of the βCH_2 resonances of the major and minor conformations at 4 °C, the population of the minor conformation was estimated to be between 10 and 25% at 68 °C, and since the line broadening observed at 50 °C can only be explained when at least 15% of the protein assumes the minor conformation, this initial estimate of the population of m in BPTI(G36S) over the temperature range from 50 to 68 °C was adjusted to 20 ± 5%. This value is in agreement with the trend to increased population of the minor conformation at higher temperature evidenced by the exchange rate constants measured between 4 and 20 °C (see below).

In BPTI, the population of the minor conformer at 68 °C was estimated to be 8 ± 1%. This estimate was based on the β-proton chemical shifts of Cys 38 observed between 36 and 68 °C, and the assumptions that the chemical shift differences between major and minor conformations are temperature-independent and similar to those in BPTI(G36S). The fact that the population of the minor conformation increases with temperature is also supported by the extent of the line broadening observed at 50 and 68 °C, which is of the order of 20–40 Hz. This is much larger than what could be expected for any value of the exchange rate in the presence of only 2% of the minor conformation.

From the ratio of the populations of the minor and major conformations, [m]/[M], at 4 and 68 °C, equilibrium enthalpies, ΔH, and equilibrium entropies, ΔS, were estimated using the relation

$$-RT \ln \frac{[\mathrm{m}]}{[\mathrm{M}]} = \Delta H - T\Delta S \qquad (2)$$

where R is the gas constant and T the absolute temperature. The results are listed in Table II. Equation 2 can also be used to estimate the populations at intermediate temperatures from the population ratios at 4 and 68 °C, whereby it is implicitly assumed that ΔH and ΔS are temperature-independent.

Measurements of the Frequency of Disulfide Bond Interconversions. The exchange rate constants k_M and k_m of the equilibrium of eq 1 were determined in the temperature range between 4 and 68 °C. In the temperature range 4–20 °C this was achieved with [^{15}N,^1H]-two-spin-order exchange experiments (Wider et al., 1991). The difference of the two recorded data files is devoid of most nonexchanging direct peaks and was used for the volume integration of the exchange cross-peaks. The experiment in which the mixing time precedes the t_1-evolution period (Wider et al., 1991) retains exclusively those [^{15}N,^1H]-cross-peaks that are also present in a conventional [^{15}N,^1H]-COSY spectrum. It was used to

Table II: Equilibrium Enthalpies, Equilibrium Entropies, Activation Enthalpies, and Activation Entropies for the Interconversion of the Chirality of the Disulfide Bond Cys 14–Cys 38 in BPTI and BPTI(G36S) Measured at Low Temperature[a]

parameter	BPTI	BPTI(G36S)
ΔH (kcal mol^{-1})	-0.5 ± 0.8[b]	0.8 ± 1.3[c]
ΔS (cal mol^{-1} K^{-1})	10.2 ± 3.2[b]	0.4 ± 4.8[c]
$\Delta H^{\ddagger}$ (kcal mol^{-1})		
M → m	13.0 ± 3.7[d]	11.6 ± 2.3[d]
M ← m	9.4 ± 5.9[d]	9.3 ± 2.4[d]
$\Delta S^{\ddagger}$ (cal mol^{-1} K^{-1})		
M → m	-13.9 ± 13.3[d]	-13.3 ± 8.3[d]
M ← m	-18.7 ± 20.8[d]	-18.1 ± 8.5[d]

[a] Measured at pH 4.6. The activation parameters were determined in the temperature range 4–20 °C. [b] From the equilibrium constants at 4 °C (population of the minor conformer 1.5 ± 0.3%) and at 68 °C (8 ± 1%). [c] From the equilibrium constants at 4 °C (population of the minor conformer (14.4 ± 2.0%) and at 68 °C (20 ± 5%). [d] The error ranges were determined from the steepest and least steep slopes compatible with the error bars indicated in Figure 10.

measure the volume integral, I, of the direct correlation peaks. For BPTI(G36S), spectra were recorded with mixing times, τ_{mix}, of 15, 30, 45, and 60 ms at 4 °C, τ_{mix} = 5, 15, 25, and 35 ms at 10 °C, and τ_{mix} = 5 and 10 ms at 7, 13, and 16 °C. The exchange rate constants k were determined from the initial buildup rates of the exchange cross-peaks in the difference spectrum, $\Delta I/\Delta\tau_{mix}$, and the intensities of the direct correlation peaks at zero mixing time, I_0:

$$k = \Delta I/(I_0 \Delta\tau_{mix}) \quad (3)$$

To avoid the recording of separate experiments with zero mixing time, I_0 was obtained by extrapolation from the data recorded with short mixing times, assuming that the decay can be described by a single exponential.

In this procedure an important correction had to be made, since with increasing temperatures the exchange rates became sufficiently rapid for the chemical exchange during the refocusing delay, τ, between evolution and detection to cause the appearance of exchange peaks even in a conventional [^{15}N,^{1}H]-COSY spectrum. The refocusing delay τ used in the [^{15}N,^{1}H]-two-spin-order exchange experiments was about 5.4 ms. To account for the effective transverse relaxation caused by the chemical exchange during τ, which is different for the major and minor conformations, we corrected the peak intensities observed at the chemical shifts of the major and minor components by $\exp(k_m\tau)$ and $\exp(k_M\tau)$, respectively. Since initially only approximate values of the exchange rate constants k_m and k_M were available from the spectral analysis without correction for the exchange during τ, this correction was applied repeatedly, where in each subsequent cycle the new, improved rate constants were used until no further change in the k_m and k_M values was observed. The final, thus corrected rate constants differed by up to 26% from the rate constants obtained without this correction.

Because the low abundance of the minor conformation in wild-type BPTI required exceptionally long recording times for its detection, [^{15}N,^{1}H]-two-spin-order exchange experiments at 10 and 16 °C were recorded with only two different mixing times, 7.5 and 15 ms, and at 4, 7, and 13 °C only a single mixing time of 10 ms was used to evaluate the exchange rates in BPTI. The results obtained with mixing times of 7.5 and 15 ms showed that τ_{mix} = 10 ms was sufficiently short to approximate the initial-rate condition, where the volumes of the exchange cross-peaks are directly proportional to the exchange rates. Furthermore, with BPTI(G36S) it was observed that during the mixing time all direct correlation peaks relax to a similar degree at all temperatures. Therefore, it was assumed that the same amount of relaxation as in BPTI(G36S) occurs also for the direct correlation peaks in BPTI, and a corresponding correction was applied to obtain the I_0 value for those temperatures where only a single mixing time was used. For τ_{mix} = 10 ms, this correction factor was 1.12.

At low plot levels most of the direct cross-peaks of the minor conformations overlap with wings of other peaks in the [^{15}N,^{1}H]-COSY spectrum, which prohibits their accurate integration. In addition, different transverse relaxation rates during the defocusing and refocusing delays of the [^{15}N,^{1}H]-two-spin-exchange experiment resulted in different intensities of the exchange patterns observed for the different amino acid residues. Therefore, the rate constants were determined only from the cross-peaks of Cys 14 and Ala 16 in BPTI(G36S) and from the relatively intense [^{15}N,^{1}H] cross-peaks of Ala 16 in BPTI. The measured exchange lifetimes ranged from about 16 ms for the minor conformation of BPTI(G36S) at 16 °C to 4.5 s for the major conformation of BPTI at 4 °C.

Above room temperature the evaluation of the exchange rate constants by this approach was made difficult by the aforementioned line broadening and the correspondingly reduced heights of the exchange peaks at the short mixing times needed to maintain the initial rate condition. In this limit, more accurate results for BPTI(G36S) were obtained by comparing the line widths of the minor and major conformations from spectra recorded with good signal-to-noise ratio. The line widths were obtained from the difference spectra and the reference spectra of [^{15}N,^{1}H]-two-spin-order exchange experiments recorded at 16 °C using a mixing time of 15 ms and a total recording time of 3 h and at 20 °C using a mixing time of 5 ms and a recording time of 9 h. Since the two conformations are present in different amounts, the chemical exchange leads to more severe line broadening in the minor form than in the major form. Assuming the same natural line width for both conformations, the difference of the full line widths at half-height of the minor and major conformations, $\Delta\nu_m - \Delta\nu_M$, is proportional to the difference in the rate constants k_M and k_m of the equilibrium of eq 1 and independent of the natural line width:

$$\Delta\nu_m - \Delta\nu_M = \frac{k_m - k_M}{\pi} \quad (4)$$

Using

$$k_m = \frac{[M]}{[m]} k_M \quad (5)$$

eq 4 can be rewritten as

$$k_M = \pi \frac{(\Delta\nu_m - \Delta\nu_M)}{\frac{[M]}{[m]} - 1} \quad (6)$$

The exchange rate constants k_m and k_M were determined from eqs 5 and 6. A critical point in the data evaluation is the accurate determination of the ratio of the major versus the minor conformation, [M]/[m]. Since no signals from the minor conformation could be resolved in the one-dimensional ^{1}H or ^{15}N NMR spectra, this ratio was determined from the antiphase signals in two-dimensional [^{15}N,^{1}H]-COSY spectra recorded without refocusing of the heteronuclear antiphase magnetization, since any chemical exchange occurring during a refocusing delay would decrease [m] more than [M] (see above). At 16 °C the exchange rate constants measured from such line width comparisons agreed well with the rate constants determined from the buildup rates of the exchange cross-peaks. At lower temperatures and correspondingly slower

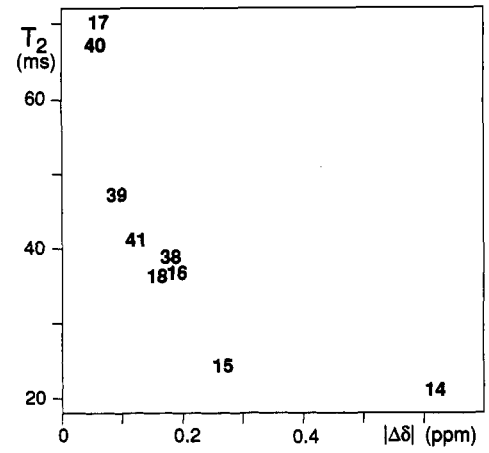

FIGURE 9: Plot of the T_2 relaxation times of the amide protons of residues 14–18 and 38–41 in BPTI versus the absolute ^1H chemical shift difference between the major and minor conformations (Table I). The T_2 values were obtained from a nonlinear fit of the cross-peak intensities observed in a set of J-modulated [^{15}N,^1H]-COSY experiments recorded at a ^1H frequency of 500 MHz with uniformly ^{15}N-enriched BPTI at 36 °C and pH 4.6. No data are given for glycyl residues, because from the experiments used no reliable T_2 values can be extracted for systems with two $^3J_{HN\alpha}$ coupling constants (Billeter et al., 1992).

exchange rates, the line width comparison yielded less accurate results, because the lines broadened too little compared with their natural line widths.

Because of the shorter lifetime, the resonances of the minor conformation broaden more rapidly with increasing temperature than those of the major conformation. Once the signals of the less abundant conformation are too broad to be detected, only the resonance lines of the major conformation can be monitored to extract the exchange rate constants. Similarly, above the coalescence temperature, only a single, average signal is observable. At 50 and 68 °C, where we had this situation, estimates of the exchange rate constants were obtained from the line widths of the $C^\beta H_2$ resonances of Cys 38 by comparison with values simulated for a range of exchange rates using the equilibrium constants determined at these temperatures. Since both β-protons change their chemical environment simultaneously during a disulfide flip, the predicted parameters could be checked against two different experimental line width measurements.

In BPTI(G36S) the β_2- and β_3-proton resonances of Cys 38 broaden by about 200 and 100 Hz at 50 °C, respectively. The same signals are only about half as broad at 68 °C. With a population of the minor conformation of 20 ± 5%, these line widths indicate exchange frequencies k_M of the disulfide flip of between 500 and 1000 s^{-1} at 50 °C and between 2000 and 6000 s^{-1} at 68 °C. The corresponding exchange line broadenings in BPTI were between 20 and 40 Hz at 68 °C. Using a population of the minor conformer of 8 ± 1% at 68 °C, the observed line broadenings correspond to a rate constant k_M of the order of 2000–3000 s^{-1} at 68 °C.

A further estimate of the exchange rate constant k_M for BPTI at 36 °C was obtained from the T_2 relaxation times of the amide protons involved in the exchange patterns of Figure 3. The T_2 relaxation times of the amide protons were obtained as a by-product of the determination of the scalar coupling constants $^3J_{HN\alpha}$ in uniformely ^{15}N-enriched BPTI from a series of J-modulated [^{15}N,^1H]-COSY spectra (Neri et al., 1990; Billeter et al., 1992). Strikingly, T_2 relaxation times shorter than 50 ms were observed exclusively for those residues which are affected by the disulfide flip in BPTI. Figure 9 shows that there exists an inverse correlation between the T_2 relaxation times of the rapidly relaxing amide protons and the ^1H chemical shift differences between the amide proton resonances of the major and minor conformations (Figure 3). A special case is presented by Tyr 35, which is not present in Figure 9. For the amide proton of Tyr 35, a T_2 relaxation time of 44 ms was determined. According to Figure 9, this value would correspond to a $\Delta\delta$ value of about 0.1 ppm, which should be sufficiently large for the observation of a well-resolved exchange pattern in the [^{15}N,^1H]-two-spin-exchange difference experiment (Figures 2 and 3). Although Tyr 35 gives rise to an exchange pattern in BPTI(G36S) (Figure 2), no such pattern was detected in the corresponding exchange spectrum of BPTI (Figure 3), which might be explained by degenerate ^{15}N chemical shifts in the minor and major conformations. Interpolation between the equilibrium populations at 4 and 68 °C based on eq 2 predicts the population of the minor form to be about 4% at 36 °C. Attributing the increased T_2 relaxation rates of the residues included in Figure 9 to the disulfide bond isomerization, the above population of the minor conformation, the chemical shifts of Figure 3 and a natural line width corresponding to T_2 = 70 ms were used to simulate the theoretical line widths for a range of different exchange rate constants using the analytical equation for a two-side exchange system with different populations at both sites (Gutowsky & Holm, 1956). The rate constant k_M obtained in this way was of the order of 40 ± 20 s^{-1}.

Activation parameters were determined in the temperature range 4–20 °C, where the exchange rates could be measured directly from [^{15}N,^1H]-two-spin-exchange experiments. The rate constants, k, determined at the different temperatures, T, were converted into ratios of free activation energies over the temperature, $\Delta G^\ddagger/T$, according to the Eyring theory:

$$\frac{\Delta G^\ddagger}{T} = -R\left(\ln k + \ln \frac{h}{\kappa k_B T}\right) \quad (7)$$

In eq 7, h denotes the Planck constant, k_B the Boltzmann constant, and κ the transmission coefficient, which was assumed to be unity over the entire temperature range used. Figure 10 shows a plot of $\Delta G^\ddagger/T$ versus $1/T$. Activation enthalpies, $\Delta H^\ddagger$, and activation entropies, $\Delta S^\ddagger$, were determined from the slopes and the intersections with the ordinate according to

$$\frac{\Delta G^\ddagger}{T} = \frac{\Delta H^\ddagger}{T} - \Delta S^\ddagger \quad (8)$$

Table II affords a survey over the activation parameters. The error ranges were obtained by fitting straight lines through the data points, assuming that the flattest and the steepest slopes compatible with the error bars in Figure 10 represent the uncertainties of the measurements. For BPTI(G36S), very similar exchange rate constants were determined from the cross-peaks of Cys 14 and Ala 16, as one would expect for a two-state equilibrium according to eq 1, where all protons change their chemical environment simultaneously.

Figure 10 shows that for both BPTI and BPTI(G36S) the differences between the free energies of activation of the forward reaction, M → m, and the backward reaction, m → M, in eq 1 decrease with increasing temperature. From the corresponding ratios k_m/k_M, the population of the minor conformation of BPTI was found to increase from 1.5% to 2.2% in the temperature range 4–16 °C. The corresponding increase in BPTI(G36S) was from 14% at 4 °C to 17% at 20 °C. The equilibrium constants determined from the ratios of the exchange rate constants agree well with the values determined independently from the intensity ratios of the direct [^{15}N,^1H]-COSY cross-peaks observed for the minor and major conformations. This result indicates that in the temperature

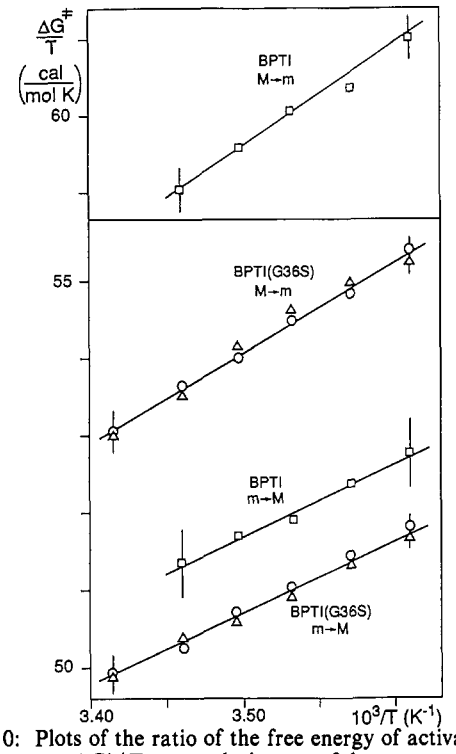

FIGURE 10: Plots of the ratio of the free energy of activation over the temperature, $\Delta G^{\ddagger}/T$, versus the inverse of the temperature, $1/T$, for the forward reaction of eq 1, M → m, and the backward reaction, M ← m, in BPTI and BPTI(G36S). The data were obtained from the ^{15}N–^{1}H cross-peaks of Ala 16 (squares and triangles) and from Cys 14 (circles). The error bars associated with the peripheral data points were obtained from error propagation, with the assumption of ±10% error in the volume integration or ±1.5 Hz error in the line width measurements. An error range of ±20% was attributed to the I_0 value of the minor conformation in BPTI in eq 3.

range between 4 and 20 °C, the exchange reaction proceeds via a single transition state, as expressed by eq 1.

DISCUSSION

Kinetic measurements with small organic model compounds have shown that the free energies of activation, $\Delta G^{\ddagger}$, for the exchange between the two different disulfide bond chiralities are of the order of 7–8 kcal/mol at temperatures around −100 °C (Fraser et al., 1971). This activation barrier is only about half of the free energy of activation for the disulfide flip Cys 14–Cys 38 in BPTI and BPTI(G36S). Correspondingly, no multiple conformers of free cystine in aqueous solution can be separately observed by NMR, and the particularly strongly constrained *cyclo*-L-cystine is the only low molecular weight compound for which the free energy of activation was found to be as high as 15.6 kcal/mol (Jung & Ottnad, 1974). These considerations show clearly that the observed slow exchange of the disulfide chirality in BPTI cannot be explained by the local covalent structure and must be due to steric constraints imposed by the protein environment.

The following considerations provide some indications why only one of the three disulfide bonds in BPTI shows slow interchange between two observably populated conformations. The disulfide flips of Cys 14–Cys 38 are coupled with minimal rearrangements of the rest of the protein molecule. Visual inspection of the other disulfide bonds in BPTI shows that a similar change of chirality would induce much larger changes of the average three-dimensional structure, so that the corresponding equilibria largely favor one of the two disulfide bond chiralities. The Cys 14–Cys 38 bond is also unique among the disulfide bonds in BPTI in that the χ^1 angle of 60° for Cys 38 in the major conformation places the sulfur atom in a sterically unfavorable position between the main chain atoms of Cys 38 (Figure 7; Richardson, 1981; Srinivasan et al., 1990). The change to a χ^1 angle of −60° in the minor conformation releases this local strain, which might contribute to the significant population of the minor conformational state.

Further insights into the special role of the Cys 14–Cys 38 bond might also derive from the fact that the minor conformation is more abundant in BPTI(G36S) than in BPTI. In the crystal structure of BPTI, an interior water molecule located near the disulfide bond Cys 14–Cys 38 is hydrogen-bonded to the carbonyl-oxygen of Cys 38. In BPTI(G36S) the hydroxyl group of Ser 36 replaces this water molecule and forms hydrogen bonds with the same partners (Berndt et al., 1993). However, because of steric constraints arising from the covalent attachment to the Ser side chain, it cannot approach the carbonyl oxygen of Cys 38 as closely as does the water molecule in BPTI. The ensuing change of the hydrogen bond to Cys 38 might explain that the proton chemical shift differences between the major and minor conformations of BPTI and BPTI(G36S) are significantly different near this residue (Figure 8a). A change in the hydrogen-bonding pattern would not be expected to be reflected in the ^{15}N chemical shifts (Figure 8b), since these are rather insensitive to hydrogen bonding (Glushka et al., 1989).

The proximity of the aromatic side chain of Tyr 35 to the disulfide bridge Cys 14–Cys 38 raises the question whether there might be some coupling between the presently described disulfide flips and the previously characterized 180° flips of this aromatic ring (Wagner et al., 1976). To enable a comparison between the different motional modes in BPTI and BPTI(G36S), we measured the ring flip frequencies of Tyr 35 in BPTI(G36S) and in BPTI with two-dimensional exchange experiments (Fejzo et al., 1990). These measurements yielded more accurate rate constants than could previously be obtained from the line-shape analysis in one-dimensional ^{1}H NMR spectra (Wagner et al., 1976). The ring flip rates of Tyr 35 in BPTI at 26, 40, and 50 °C were found to be $1.3 \pm 0.2\ s^{-1}$, $16 \pm 1\ s^{-1}$ and $80 \pm 20\ s^{-1}$, respectively, and in BPTI(G36S) the corresponding ring flip rates were about twice these values. From the temperature dependence of the ring flip rates, the activation parameters $\Delta H^{\ddagger}$ and $\Delta S^{\ddagger}$ in BPTI were determined to be about 33 kcal/mol and 53 cal/mol K, respectively. A survey of the kinetic results obtained for the aromatic ring flips of Tyr 35 and the disulfide flips in BPTI and BPTI(G36S) (Figure 11) indicates that the ring flips and the disulfide flips are not correlated at temperatures below room temperature. Their different nature is reflected in the significantly smaller free energies of activation for the disulfide flips (Figure 11). With increasing temperature, however, the disulfide flip rates increase much more rapidly than anticipated from the low temperature data of Table II. For example, on the basis of these activation parameters, rate constants k_M in the range of 10–70 s^{-1} and 150–600 s^{-1}, respectively, would be predicted for BPTI and BPTI(G36S) at 68 °C. The experimentally observed rate constants, however, are faster by one order of magnitude or more. This implies that the disulfide flip rates do not follow an Arrhenius-type temperature dependence over the entire range from 4 to 68 °C. Yet the temperature dependence of the equilibrium constants is still in line with the predictions from Figure 10. For example, using the curves drawn in Figure 10 and eqs 2 and 5, the population of the minor conformation in BPTI is estimated to be about 6% at 68 °C, which coincides closely with the value of 8% obtained from the averaged chemical shift of the β_2H–β_3H cross-peaks of Cys 38. The situation of the accelerated reaction rates at the higher

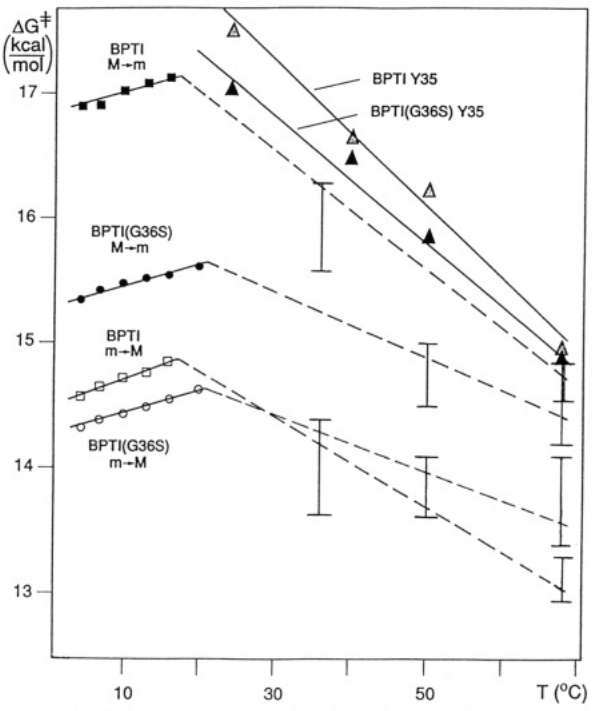

FIGURE 11: Plots of the free energies of activation, $\Delta G^{\ddagger}$, versus the temperature, T, for the forward reaction of eq 1, M → m, and the backward reaction, M ← m, in BPTI and BPTI(G36S). The data in the temperature range 4–20 °C are taken from Figure 10. Above 20 °C, vertical vars at 36, 50, and 68 °C, respectively, indicate the ranges of $\Delta G^{\ddagger}$ values that are compatible with the T_2 relaxation data of the amide protons of BPTI at 36 °C, the β-proton line widths of Cys 38 in BPTI(G36S) at 50 °C, and the β-proton line widths of Cys 38 in BPTI(G36S) and BPTI at 68 °C (see the text). To indicate the general trend, these large uncertainty ranges are connected by dashed lines. Also indicated with black and shaded triangles connected by solid lines are the $\Delta G^{\ddagger}$ values measured for the 180° ring flips of Tyr 35 in the two proteins (see the text).

temperatures with unchanged equilibrium parameters can be rationalized as intramolecular catalysis of the disulfide flips by local structure fluctuations similar to those manifested by the ring flips of Tyr 35.

It is intriguing to note that the disulfide flip rates k_M in BPTI and BPTI(G36S) are faster than the Tyr 35 ring flip rates over the entire temperature range from 4 to 68 °C. Using the activation parameters of the Tyr 35 ring flip, the flip rate at 4 °C is calculated to be 0.015 s^{-1}, which is too slow to be measured by ^{1}H NMR spectroscopy. The disulfide flip in BPTI occurs with much faster rates at this temperature, i.e., k_M = 0.27 s^{-1} and k_m = 16.8 s^{-1}, and even faster rates are observed in BPTI(G36S) (Figure 10). Thus, at low temperature the disulfide flips proceed much more easily than the Tyr 35 ring flips. On the basis of the activation parameters of the two different motions, the Tyr 35 ring flip rate would be expected to become faster than the disulfide flip rate at temperatures between 25 and 50 °C. The fact that the disulfide flip rates are actually faster over the entire temperature range implicates that above room temperature both NMR-detectable motions are triggered by similar structure fluctuations of the protein. A similar conclusion comes from the activation parameters $\Delta H^{\ddagger}$ and $\Delta S^{\ddagger}$ of the disulfide flip estimated from the rate constants k_M at 16 and 68 °C, which are more similar to the activation parameters of the Tyr 35 ring flip than to the parameters of Table II, with a positive value of the activation entropy, $\Delta S^{\ddagger}$.

In addition to the interest relative to protein structure and dynamics, the question arises whether the disulfide flips could interfere with the inhibitory binding of BPTI to trypsin. As it was observed earlier that selective reduction of the Cys 14–Cys 38 disulfide bond results in virtually unaltered binding affinity to trypsin (Kress et al., 1968), the strictly local changes coupled with the disulfide flips (Figure 7) make a significant influence on the functional properties rather unlikely.

In conclusion, the change in chirality of the disulfide bond Cys 14–Cys 38 proceeds with an ease that may be surprising in view of the conformational restraints imposed by the three-dimensional structure of a protein as rigid as BPTI. Therefore, flipping disulfide bonds may occur more frequently in protein solutions than what might be anticipated from the usually static model representations of protein structures. The present detailed analysis of structure, equilibrium, and kinetics of a disulfide flip in BPTI lead to the characterization of an example of intramolecular catalysis of conformational exchange in a protein. It seems plausible from this investigation that the activation parameters measured at high temperatures for different conformational exchange processes in proteins reflect quite generally the energy barrier of structural fluctuations involving entire protein subdomains rather than the energy barrier for specific, locally confined conformation changes.

ACKNOWLEDGMENTS

We thank Dr. L. P. M. Orbons for measuring the T_2 relaxation times of BPTI used in Figure 9, Bayer Leverkusen, Germany, for a generous gift of uniformly ^{15}N-labeled BPTI and BPTI(G36S), and Mr. R. Marani for the careful processing of the text.

SUPPLEMENTARY MATERIAL AVAILABLE

One table containing a survey of the data on the equilibrium and exchange rates between the two interconverting conformers observed in solutions of BPTI and BPTI(G36S) (2 pages). Ordering information is given on any current masthead page.

REFERENCES

Bax, A., Ikura, M., Kay, L. E., & Zhu, G. (1991) *J. Magn. Reson. 91*, 174–178.

Berndt, K. D., Güntert, P., Orbons, L. P. M., & Wüthrich, K. (1992) *J. Mol. Biol. 227*, 757–775.

Berndt, K. D., Beunink, J., Schröder, W., & Wüthrich, K. (1993) *Biochemistry* (in press).

Billeter, M., Neri, D., Otting, G., Qian, Y. Q., & Wüthrich, K. (1992) *J. Biomol. NMR 2*, 257–274.

Bodenhausen, G., & Ruben, D. J. (1980) *Chem. Phys. Lett. 69*, 185–189.

Bothner-By, A. A., Stephens, R. L., Lee, J., Warren, C. D., & Jeanloz, R. W. (1984) *J. Am. Chem. Soc. 106*, 811–813.

Chazin, W. J., Goldenberg, D. P., Creighton, T. E., & Wüthrich, K. (1985) *Eur. J. Biochem. 152*, 429–437.

Deisenhofer, J., & Steigemann, W. (1975) *Acta Crystallogr. B 31*, 238–250.

Donzel, B., Kamber, B., Wüthrich, K., & Schwyzer, R. (1972) *Helv. Chim. Acta 55*, 947–961.

Fejzo, S., Westler, W. M., Macura, S., & Markley, J. (1990) *J. Am. Chem. Soc. 112*, 2574–2577.

Fraser, R. R., Boussard, G., Saunders, J. K., Lambert, J. B., & Mixan, C. E. (1971) *J. Am. Chem. Soc. 93*, 3822–3823.

Glushka, J., Lee, M., Coffin, S., & Cowburn, D. (1989) *J. Am. Chem. Soc. 111*, 7716–7722.

Grathwohl, C., & Wüthrich, K. (1981) *Biopolymers 20*, 2623–2633.

Griesinger, C., Otting, G., Wüthrich, K., & Ernst, R. R. (1988) *J. Am. Chem. Soc. 110*, 7870–7872.

Gutowsky, H. S., & Holm, C. H. (1956) *J. Chem. Phys. 25*, 1228–1234.

Jung, G., & Ottnad, M. (1974) *Angew. Chem. 86*, 856–857.

Kopple, K. D., Wang, J., Cheng, A. G., & Bhandary, K. K. (1988) *J. Am. Chem. Soc. 110*, 4168–4176.
Kress, L. F., Wilson, K. A., & Laskowski, M., Sr. (1968) *J. Biol. Chem. 243*, 1758–1762.
Macura, S., Wüthrich, K., & Ernst, R. R., (1982) *J. Magn. Reson. 46*, 269–282.
Marion, D., Ikura, M., Tschudin, R., & Bax, A. (1989) *J. Magn. Reson. 85*, 393–399.
Messerle, B. A., Wider, G., Otting, G., Weber, C., & Wüthrich, K. (1989) *J. Magn. Reson. 85*, 608–613.
Neri, D., Otting, G., & Wüthrich, K. (1990) *J. Am. Chem. Soc. 112*, 3663–3665.
Otting, G., & Wüthrich, K. (1988) *J. Magn. Reson. 76*, 569–574.
Otting, G., & Wüthrich, K. (1989) *J. Am. Chem. Soc. 111*, 1871–1875.
Rance, M., Sørensen, O. W., Bodenhausen, G., Wagner, G., Ernst, R. R., & Wüthrich, K. (1983) *Biochem. Biophys. Res. Commun. 117*, 479–485.
Richardson, J. S. (1981) *Adv. Protein Chem. 34*, 167–330.
Richarz, R., Nagayama, K., & Wüthrich, K. (1980) *Biochemistry 19*, 5189–5196.
Srinivasan, N., Sowdhamini, R., Ramakrishnan, C., & Balaram, P. (1990) *Int. J. Pept. Protein Res. 36*, 147–155.
Vanmierlo, C. P. M., Darby, N. J., Neuhaus, D., & Creighton, T. E. (1991) *J. Mol. Biol. 222*, 373–390.
Wagner, G. (1980) *FEBS Lett. 112*, 280–284.
Wagner, G., & Wüthrich, K. (1982) *J. Mol. Biol. 155*, 347–366.
Wagner, G., & Nirmala, N. R. (1989) *Chem. Scr. 29A*, 27–30.
Wagner, G., DeMarco, A., & Wüthrich, K. (1976) *Biophys. Struct. Mech. 2*, 139–158.
Wagner, G., Stassinopoulou, C. I., & Wüthrich, K. (1984) *Eur. J. Biochem. 143*, 431–436.
Wagner, G., Braun, W., Havel, T. F., Schaumann, T., Gō, N., & Wüthrich, K. (1987) *J. Mol. Biol. 196*, 611–639.
Wider, G., Neri, D., & Wüthrich, K. (1991) *J. Biomol. NMR 1*, 93–98.
Wlodawer, A., Walter, J., Huber, R., & Sjölin, L. (1984) *J. Mol. Biol. 193*, 145–156.
Wlodawer, A., Nachman, J., Gilliland, G. L., Gallagher, W., & Woodward, C. (1987) *J. Mol. Biol. 198*, 469–480.
Wüthrich, K. (1976) *NMR in Biological Research: Peptides and Proteins*, North Holland, Amsterdam.
Wüthrich, K. (1986) *NMR of Proteins and Nucleic Acids*, Wiley, New York.